PV Powered One Stop Station for Electronic Gadget

Sahpo Delmini[1]

[1] *Vaal University of Technology*

---**ABSTRACT**---
Smartphones and small battery-powered devices are extremely essential in the present day, which have improved people's communication, entertainment and various daily tasks. However, with the widespread usage of these devices, a significant consumption of electricity can be noticed. Additionally, traditional charging methods rely on non-renewable energy sources, which can lead to a negative impact on the environment such as resource depletion, greenhouse gas emission and various pollution. But it is unavoidable that the demand for these devices will continue to grow due to the increase of population and advancements in technology. Therefore, a critical need for sustainable charging solutions should be developed. This report presents the design and simulation of a solar-powered wireless charger. The key parts include boost converter, colpitts oscillator, operational amplifier, Class-AB amplifier, full wave rectifier, buck converter and MCU. In addition, LTSpice simulation was used to effectively model and connect these parts. MPLAB is also used in write, rewrite and debug coding in MCU through PICKIT 3.
KEYWORDS: Solar Energy, Wireless Charger, Circuit Monitoring, Wearable and Portable Applications.

Date of Submission: 17-01-2025   Date of acceptance: 31-01-2025

I.   INTRODUCTION

Solar energy is recognized for its sustainability, being a renewable resource with no adverse impact on the environment. It is a clean energy generation process without greenhouse gas emissions and pollution. Additionally, solar power systems have high flexibility as solar panels can be installed in various locations, making them easily accessible. Lastly, solar energy derived from sun's rays which means this energy resource is abundant and can continuously support energy demand. With all these benefits, solar energy has been chosen for use in the design of wireless charger in this project. This report presents on the design and simulation of a solar-powered wireless charger. The key parts include boost converter, colpitts oscillator, operational amplifier, Class-AB amplifier, full wave rectifier, buck converter and MCU. In addition, LTSpice simulation was used to effectively model and connect these parts. MPLAB also used in write, rewrite and debug coding in MCU through PICKIT 3. Throughout this project, I gained valuable insights in various design principles, including circuit optimization, power electronics and signal processing. Besides, this experience has broadened my knowledge of developing efficient and sustainable energy solutions by using advanced tools.

II.   OBJECTIVE

The objective of this project is to design and implement an eco-friendly and efficient wireless charging system for smartphones and low-power electronic devices using renewable solar energy. The system was designed to operate with a 12V input (from solar panels) and provide a stable 5V output at 1A.

The system integrated various components and technologies to achieve high efficiency and performance. LTspice was used for circuit simulation to model and optimize the design of key power conversion elements, such as the boost and buck converters, and the wireless power transfer system. The simulation allowed for the optimization of component parameters to ensure that the system operates efficiently and reliably.

The power conversion was achieved using a combination of boost and buck converters. The boost converter stepped up the 12V input to higher voltage levels required for powering various components in the system, while the buck converter regulated the output to a stable 5V for device charging. The Colpitts oscillator generated high-frequency signals used in the wireless power transfer system.

For further design, the focus will be on optimizing power transmission efficiency, enhancing signal stability, and improving thermal management. By refining coil design, aligning operating frequencies, and strengthening signal integrity, the system's reliability can be increased. Additionally, better heat dissipation

methods will be developed to prevent overheating and ensure consistent performance. Simplifying the circuit design and integrating components will reduce complexity, while moving to a custom-designed PCB will minimize size, improve portability, and enhance durability.

III. LITERATURE REVIEW

Solar Energy and Photovoltaic Cell [13][28]

Solar power system also known as Photovoltaic (PV) system which is composed of solar panel, supercapacitor and inverter. A solar panel is the component where energy conversion from sunlight to electrical energy takes places. A supercapacitor is used to store and stabilize the energy on sunny days while inverter converts generated DC electricity to AC electricity for use in household and business.
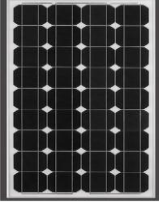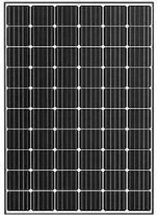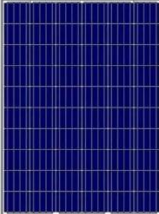
The solar panel is formed by multiply PV cells in series and parallel connection. By arranging PV cells in different configurations, desired power output requirements can be met. These PV cells are the basic units which consists of multiple layers by using p-type and n-type semiconductors. In the process of solar power generation, these layers are responsible for converting sunlight into electrical power through photovoltaic (PV) effect.

The photovoltaic (PV) effect occurs in a p-n junction, where p-type and n-type semiconductors meet, creating an electric field. Light photons energize electrons, moving them to the conduction band and generating an electric current.

PV cells are primarily composed of silicon (Si), with crystalline silicon technology achieving an efficiency of about 25% for thin-film appl. Solar energy is a key player in the renewable and eco-friendly energy sector. As a renewable resource, it harnesses the sun's power, which is abundant and inexhaustible compared to fossil fuels. Unlike conventional energy sources, solar energy does not produce greenhouse gases or other pollutants, making it a cleaner alternative for reducing our carbon footprint.

Photovoltaic cells are using in this project. A photovoltaic (PV) cell consists of multiple layers, with the most crucial being the semiconductor layer, which includes p-type and n-type materials. These layers convert sunlight into electricity via the photovoltaic effect, generating voltage or current when exposed to light.

This is a General PV system [1]. PV panel connect with a DC-to-DC boost converter provides a controllable output voltage. The output voltage and thereby its output power controlled by duty cycle of the boost converter. As the sunlight change of the day, the input voltage will be different from the output of PV panel. PWM is applied in this system to ensure a stable load output by adjusting the on-time duration (t_{on}).

Panel Type	Efficiency	Advantage	Disadvantage	Price
Monocrystalline	Up to 20%	1. High efficiency 2. High Durability 3. Aesthetically Pleasing	1. High cost	High
Mono-PERC	Up to 22%	1. High efficiency and power output 2. Excellent performance under low-light conditions	1. Highest cost 2. Production process involves a large carbon footprint	Very High
Polycrystalline	15% - 17%	1. Mid cost; affordable	1. Medium efficiency and performance 2. Average durability	Medium

Thin-Film		10% -13%	1. Low cost 2. Easily produced 3. Light weight 4. Portable and Flexible	1. Low efficiency and performance 2. Short lifespan	Low

Table III.1 Different Types of Solar Panels[14]

The properties of four different types of solar cells are compared. Mono-PERC cells have the highest efficiency but are also the most expensive. In contrast, Thin-Film cells are the cheapest but have the lowest efficiency. Based on efficiency, cost, and performance, Monocrystalline cells are the optimal choice for this project. Therefore, Monocrystalline cells solar panel have been selected

Boost Converter [8]
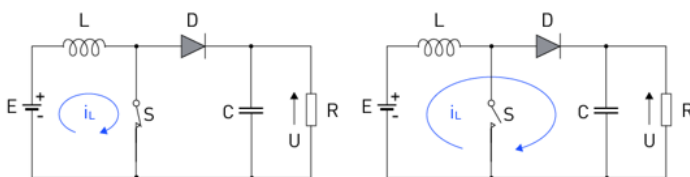
Figure III.1 Boost Converter with Switch On and Off
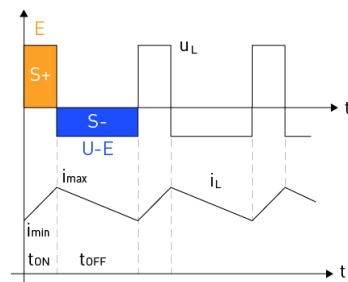
Figure III.2 Boost Converter Pulse[16]

A boost converter is a type of DC-DC converter that increases a lower input voltage to a higher output voltage. It uses an inductor, a switch, a diode, and a capacitor to step up the voltage efficiently.
PWM plays a critical role in **boost converters** by controlling the timing of the switch, which directly influences the output voltage. By carefully adjusting the duty cycle, the boost converter can efficiently step up the voltage to a desired level.
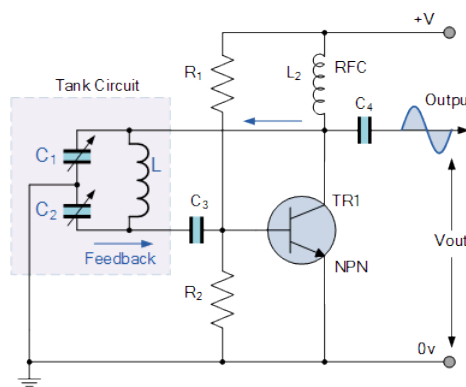
Colpitts Oscillator [9]

Figure III.3 Colpitts Oscillator Circuit

The Colpitts oscillator is a type of electronic oscillator that generates a continuous sine wave. It uses a tank circuit consisting of an inductor and two capacitors connected in series to create oscillations. The feedback for the oscillations is provided through a portion of the tank circuit, and the frequency of oscillation is determined by the values of the inductor and capacitors. It is commonly used in RF and communication circuits.
The calculation is:

$$f_o = \frac{1}{2\pi \times \sqrt{LC}}$$
$$C = \frac{C_{t1} \times C_{t2}}{C_{t1} + C_{t2}}$$

where;

C   = The Equivalent capacitance
C_1 = The value of coupled capacitor 1
C_2 = The value of coupled capacitor 2
f_o = The resonant frequency
L   = The value of coupled inductor

Class AB Amplifier [10]

Class AB is the combination of Class A and Class B, which can achieve a higher efficiency than Class A while lower distortion than Class B. This is because biasing both transistors allow the conduct when the signal is near zero.

Class A: – The amplifiers single output transistor conducts for 360o of the input waveform.
Class B: – The amplifiers two output transistors only conduct for 180o of the input waveform.
Class AB: – The amplifiers two output transistors conduct between 180o and 360o of the input waveform.
Class A amplifiers are known for their high linear performance but are less efficient, Class B amplifiers provide high efficiency at the cost of some distortion, and Class AB amplifiers provide a compromise, offering a good balance between efficiency and linearity.
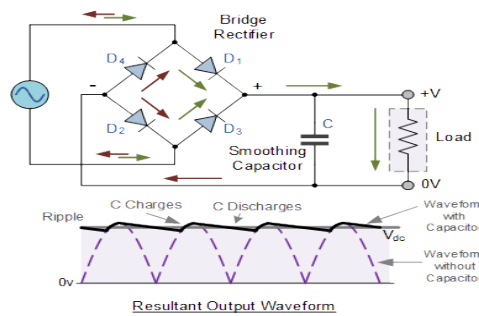
Full Wave Rectifier[17]

Figure III.4 Full Wave Rectifier Circuit

A full-wave rectifier converts AC to DC using both halves of the AC waveform. It can be a centre-tap rectifier with two diodes and a transformer, or a bridge rectifier with four diodes, providing a smoother DC output.

Buck Converter [11]

A buck converter is a DC-DC step-down converter which is developed to lower a higher input voltage to a lower output voltage. It operates by employing an inductor, a capacitor, a transistor, and a diode to ensure the voltage reduction. The transistor's switching, managed by feedback, keeps the output voltage stable despite variations in input or load. Buck converters are favoured for their efficiency and versatility in handling different voltage levels.

Wireless Power Transfer [12]

The transistor amplifier is configured as a Common Emitter Amplifier, where the output signal is 180° out of phase with the input signal. The extra 180° phase shift needed for oscillation is provided by the series connection of the two capacitors, which are placed in parallel with the inductive coil. This configuration results in the overall phase shift of the circuit being 0° or 360°.[35]

Wireless Power Transfer (WPT) networks allow electrical energy transmission without physical connection. Instead, electromagnetic fields are used to transfer the power between a transmitter and a receiver. The transmitter circuit consists of power source, oscillator, amplifier and a transmitter coil. While the receiver circuit includes a receiver coil, a rectifier, a filter to smooth the DC signal and a regulator to stabilize the DC output.

There are various methods to achieve WPT such as inductive coupling, resonant coupling, capacitive coupling and magnetic resonance. In addition, WPT has a variety of applications in wireless charging of phones, medical devices, and remote power delivery.

Op – Amp[18]

An operational amplifier (Op-amp) is a high-gain electronic amplifier commonly used in various analog circuits. Its main function is to amplify the voltage of an input signal and perform various mathematical operations, such as addition, subtraction, integration, and differentiation. An Op-amp typically has two input terminals (inverting and non-inverting) and one output terminal. External components like resistors and capacitors are used to adjust its operating state, allowing it to perform different functions. Due to its high gain, Op-amps are widely used in signal conditioning, filtering, and signal amplification.
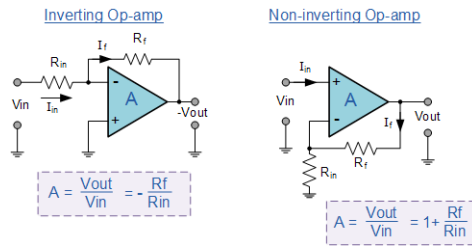
Figure III.5 Op-Amp [20]

The amplification function of an Op-amp is achieved through a feedback mechanism, especially negative feedback. With negative feedback, the relationship between the output and input signals is precisely controlled, preventing excessive amplification. By adjusting external feedback resistors, the amplification factor of the Op-amp can be easily modified. For example, in an inverting amplifier configuration, changing the value of the feedback resistor can alter the amplification factor, allowing for different gain requirements. This flexibility makes Op-amps a highly versatile and widely used electronic component.

IV. Project Overview
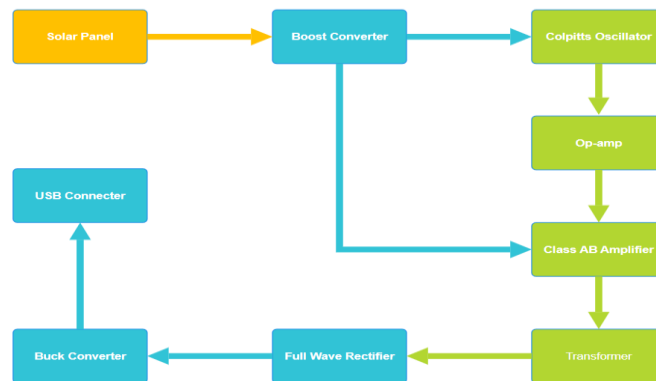
Figure IV.1 - Project Block Diagram

In this design, the solar panels supply a voltage of 12V. A boost converter converts the irregular voltage into a stable 24V DC output first and then the Colpitts oscillator can transform this DC current into AC current for wireless transmission. On the receiving end, a full-wave rectifier converts the 100kHz AC current into DC current using a parallel capacitor configuration. Lastly, the DC output is stepwise decreased to 5V at using a buck converter.

V. Design and Simulation

Colpitts Oscillator Calculation [21][22]

In this section, an amplifier transistor BJT 2N2222 is used in this simulation of Colpitts Oscillator.
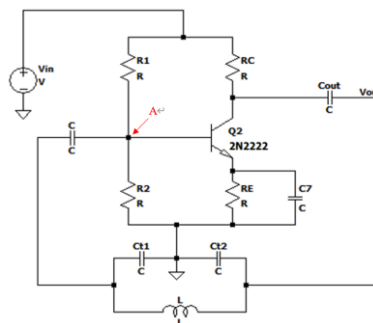

Figure V.1 - The Colpitts Oscillator Circuit Connection

Figure V.1 shows the basic circuit connection of Colpitts Oscillator Circuit. To calculate all the resistor values, this information is obtained from datasheet:

V_{BE} = 0.7V, The voltage between the Base and Emitter

h_{FEmin} = 100, The minimum dc current gain
h_{FEmax} = 300, The maximum dc current gain

Find out R_2 value, by assume the value of R_E is 1kΩ [7]:

$$R_2 \leq \frac{\sqrt{h_{FEmin} \times h_{FEmax}} \times R_E}{10}$$

By submitting values into this equation, get:

$$R_2 \leq \frac{\sqrt{100 \times 300} \times 1000}{10} = 17.3k\Omega$$

Hence, to minimise the distortion, 4kΩ can be chosen as R_2 Value. Then by applying KCL at point A:

$$I_{R1} = I_{R2} + I_B$$

As R_1 and R_2 work as a voltage divider biasing. To make sure the voltage divider and the transformer work, the current of base I_B should be as small as possible, so that current flow in R_1 will be much higher than I_B, in this case I_{R1} is slated to 50 times of I_B. [23]

$$I_{R2} = \frac{(V_{BE} + (h_{FE} + 1) \times I_B \times R_E)}{R_2}$$

$$I_{R1} = 50 \times I_B$$

$$I_C = h_{FE} \times I_B$$

Then, the calculation of I_B is:

$$50I_B = \frac{(0.7 + (173 + 1) \times I_B \times 1000)}{4000}$$

After simplifying, I_B value is:

$$I_B = \frac{(0.7 + (173 + 1) \times I_B \times 1000)}{4000} = 0.027mA$$

Hence:

$$I_{R1} = 50 \times 0.027 \times 10^{-3} = 1.35mA$$

$$I_C = 173 \times 0.027 \times 10^{-3} = 4.671mA$$

Then calculate R_2 by applying KVL on base circuit:

$$R_1 = \frac{V_{in} - V_{BE} - I_B(h_{FE} + 1) \times R_E}{I_{R1}}$$

Values were substituted in,

$$R_1 = \frac{24 - 0.7 - 0.027 \times 10^{-3}(173 + 1) \times 1000}{1.35 \times 10^{-3}} = 13.8k\Omega$$

To find out R_c value, apply KVL on collector circuit:

$$V_{CE} = V_{in} - I_c(R_c + R_E)$$

Values were substituted in,

$$3.5 = 24 - 4.671 \times 10^{-3}(R_c + 1000)$$

Simplify equation:

$$R_c = \frac{24 - 3.5 - 4.671 \times 10^{-3} \times 1000}{4.671 \times 10^{-3}} = 3.3k\Omega$$

The Equivalent capacitance of the coupled capacitors can be calculated from:

$$C = \frac{C_{t1} \times C_{t2}}{C_{t1} + C_{t2}}$$

where;

C = The Equivalent capacitance
C_{t1} = The value of coupled capacitor 1
C_{t2} = The value of coupled capacitor 2

By sub in the values of two coupled capacitors, get:

$$C = \frac{9.1 \times 10^{-8} \times 9.1 \times 10^{-8}}{9.1 \times 10^{-8} + 9.1 \times 10^{-8}} = 53.89nF$$

Hence the value of Resonant frequency is:

$$f_o = \frac{1}{2\pi \times \sqrt{LC}}$$

where;

f_o = The resonant frequency
L = The value of coupled inductor
C = The Equivalent capacitance

After sub in the values, then:

$$f_o = \frac{1}{2\pi \times \sqrt{47 * 10^{-6} \times 5.389 \times 10^{-8}}} = 100kHz$$

Hence, the simulated output signal should be sin wave signal with frequency of 100kHz.
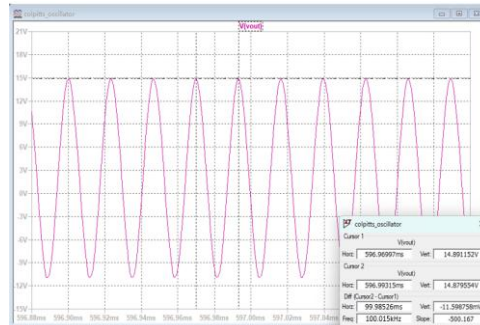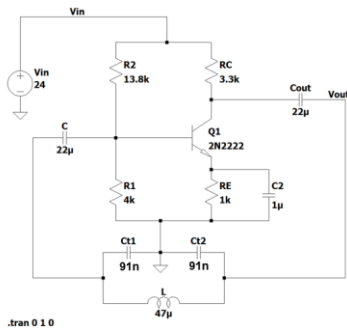
Simulation of Colpitts Oscillator

Figure V.2 - Simulation of Colpitts Oscillator   Figure V.3 - The Output Waveform of the Colpitts Oscillator

From the waveform of the output, a sign wave is be generated with frequency of 100.015kHz, amplitude of 25.6Vp-p. which is successful match the calculated value of 100kHz.

Circuit Connection of Class AB Amplifier [23]
The overall connection for class AB Amplifier is as shown below. A Class AB amplifier can amplify the original signal and output a full-waveform signal.
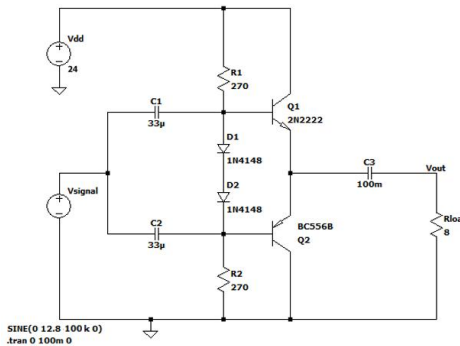
Figure V.4 The Connection of Class AB Amplifier [24]

A 24V DC power supply is used to provide power to the entire circuit. It also determines the maximum output voltage. Resistors R1 and R2 are set to 270Ω which are used for forward biasing the diodes so that they drop 0.7V across it for biasing the individual transistors. C1 and C2 are input DC decoupling capacitors, which block DC components of the input signal to ensure that only AC components pass through to the transistor bases.
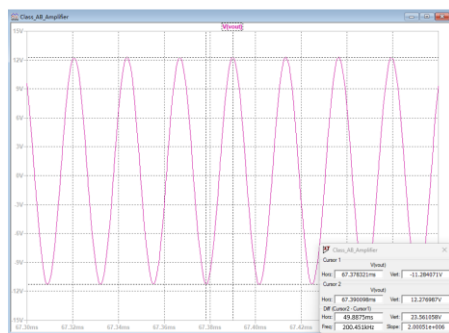**Simulation of Class AB Amplifier**

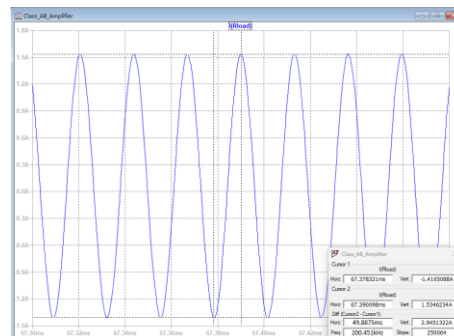Figure V.5 The Output Voltage Waveform of
Class AB Amplifier

Figure V.6 The Output Current Waveform of
Class AB Amplifier

Figure V.5 and Figure V.6 shows the output voltage form class ab amplifier is sign wave with amplitude of 23.56V peak to peak, and frequency is 200.451kHz / 2 = 100.225kHz. The output current amplitude is 1.53A peak to peak. which is meet the expect result.
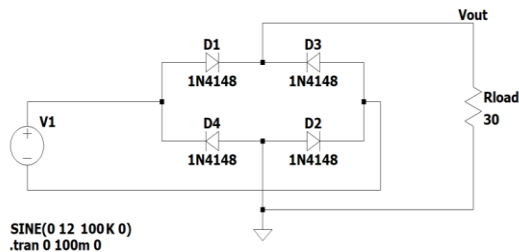
Full Wave Rectifier [26]

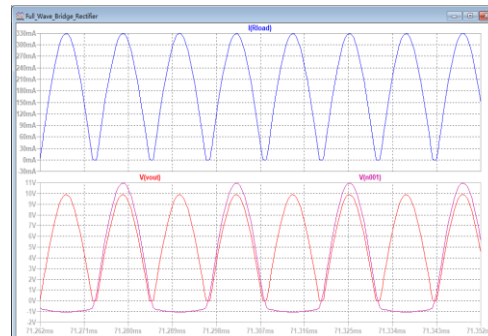Figure V.7 The Connection of Full Wave Bridge Rectifier without Capacitor

Figure V.8 The Output Voltage and Current of Full Wave Rectifier without Capacitor

The output from the full-wave bridge rectifier resembles a half-sine wave AC signal, which could introduce significant distortion into the subsequent buck converter. To convert this to a cleaner DC output, a capacitor should be installed across the load to smooth out the waveform.
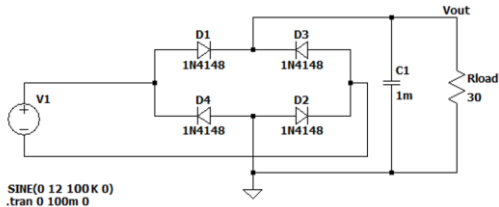

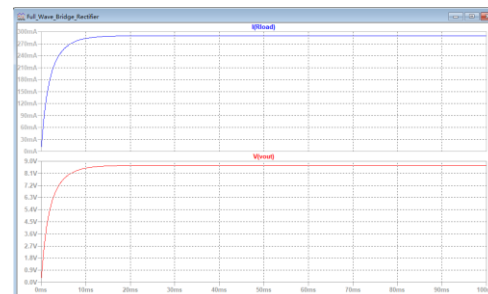Figure V.9 The Connection of Full Wave Bridge Rectifier without Capacitor

Figure V.10 The Output Voltage and Current of Full Wave Rectifier without Capacitor

The smoothing capacitor converts the full wave rippled output of the rectifier into a smoother DC output voltage. So full wave Bridge Rectifier without capacitor will used in this project.

Boost Converter IC

As a varying input into the system, the way to make output of the boost converter stable is to change the PWM signal accordingly. To better control the variations in the PWM signal, a Boost Converter IC is utilized in this project. It features a feedback loop that automatically adjusts the PWM signal frequency and duty cycle by monitoring changes in input voltage and current. Additionally, the Boost Converter IC includes an over-current protection system, enhancing the safety of the entire circuit.

Buck Converter IC (LM2596)

Since the buck converter is the last part to charging devices, its stability is very important. Overheating or damage to various components can lead to unstable output voltage. To achieve more stable output voltage, a boost converter IC LM2596 is used in this project. It can provide feedback to the circuit based on changes in the output voltage. And it can automatically adjust the time-on to control the output voltage, ensuring the stability and safety of devices.

Overall Circuit Simulation

The above is the analysis and simulation of parts of the circuits. By combining all the parts together, a simulation of the integrated load waveform and value is shown below.

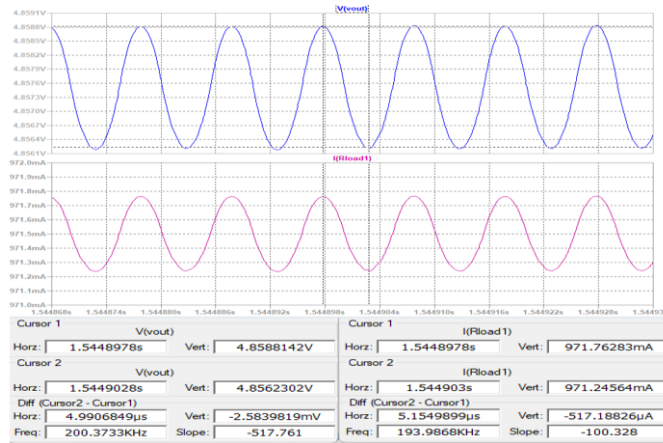The waveform obtained at load is:

Figure V.11 Waveform of Overall Circuit

From the graph V.25, it can be observed that the output voltage is around 4.85V, and the output current is approximately 971mA, which is close to the expected output values. The simulation design successfully achieves an output of 5V at 1A.

Microcontroller and LCD[33]

Microcontroller PIC18F4550 is a functional and have enhance performance. In this project, this MCU is used for voltage and current monitor, overload protection and LCD driver.

As the maximum voltage into the microcontroller is 5V, the voltage of each circuit is higher than 5V, so voltage divider is used at each monitoring point, Also the current sensor is need for monitoring current from the circuit. The following diagram shows the position of current and voltage monitoring.[41] and Microcontroller IC connection is shown below:
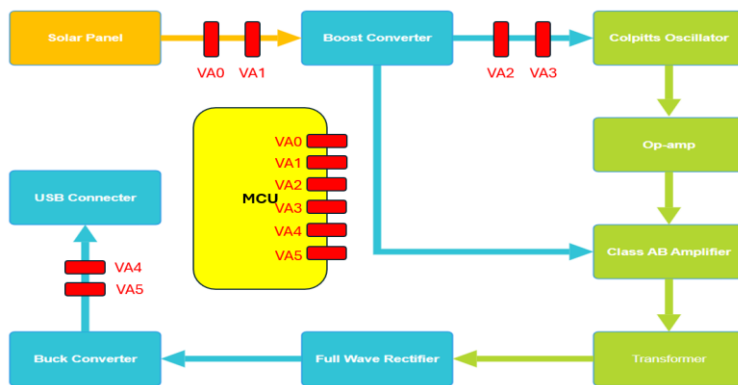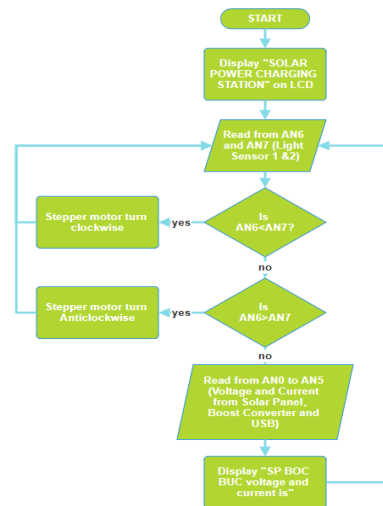

Figure V.12 The Voltage and Current Measure for MCU Monitoring Circuit Figure

V.13 The Flow Chart of MCU

With the connection of MUC, LCD is used for displaying monitored status and parameters. By getting data from LCD, allows for a clearer understanding of the charging voltage and current levels, it is easier for us to control circuit.[38]

VI. Charging System Testing

This section includes testing the basic operation of each subsystem, along with visual illustrations and data comparison tables, which enable a clear observation and understanding of the system's performance in the experiment.

Testing of Boost Converter [4][5]

In the initial design of boost converter, the conversion of DC voltage was regulated by the combination of MOSFET and a PWM control circuit. However, relatively low efficiency was observed after conducting testing and evaluation, indicating non-ideal performance. This is because MOSFET generated amount of heat during the

testing, leading to energy loss and a decrease in system efficiency. Therefore, to address this issue, Boost Converter IC LM2587 was used as an alternative. This is because it offers better thermal management, reducing heat production and energy loss, resulting in improving overall efficiency and ensure a more stable performance in voltage step-up applications. With the LM2587 integrated into the system, when a 12V DC input was applied, the output was consistently maintained at a stable 24V DC, ensuring a reliable power supply for the application. [6]

The following photos present the actual side view of the boost converter, showing the physical arrangement of components, as well as the output waveform, which demonstrates the stable 24V DC output.
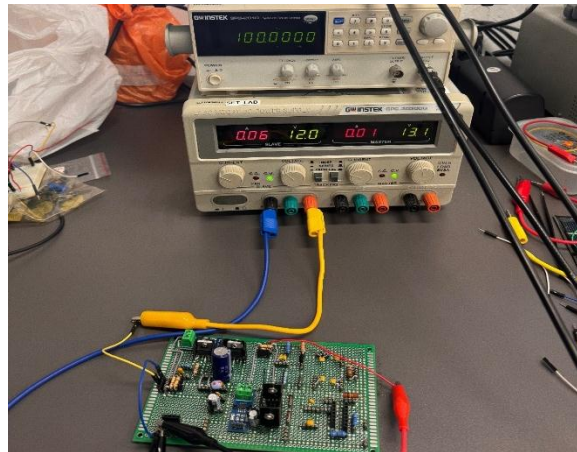

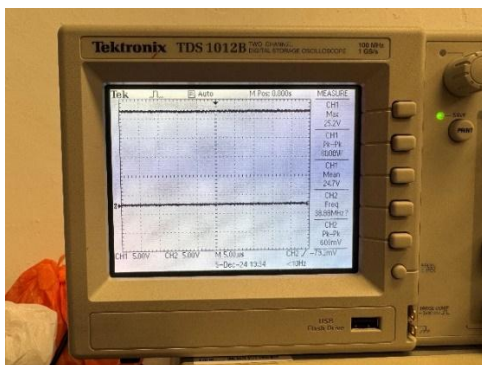Figure VI.1 Boost Converter Overall Circuit Testing [15]

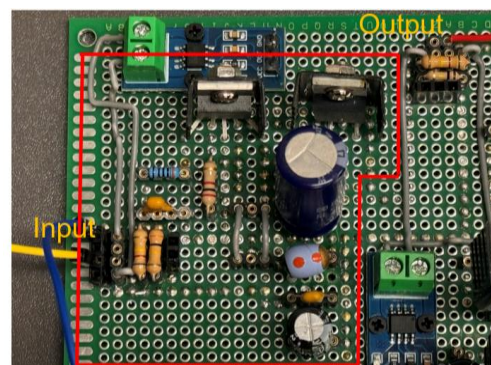Figure VI.2 Boost Converter Output Waveform

Figure VI.3 Boost Converter Soldering Board Layout

Testing of Colpitts Oscillator[29]

In the design of the Colpitts Oscillator, the first step was to determine the optimal operating frequency of the transformer, as this will directly influence the efficiency and performance of the entire system. Like boost converter testing, energy loss and heat generation were also considered during the design process. To meet the requirement, a series of tests were conducted to evaluate the transformer's performance across a range of frequencies. These tests helped to identify the frequency at which the transformer can operate most efficiently.

The following sections present the detailed results from these tests, including the relationship between the transformer's operating frequency and its efficiency. Various parameters such as input power, output power, and the resulting efficiency at different frequencies from 10kHZ to 150kHz were measured individually and recorded in table VI.1. It can be observed that at frequency of 100kHZ, the transformer can operate at a relatively high efficiency of 23%. This result indicated that at this frequency, the design has least energy loss, and the performance of the various circuit components is optimized, ensuring stable oscillation output and improved signal quality. Therefore, the most suitable frequency of 100kHz was selected for the design of Colpitts Oscillator, which will contribute to the overall system's efficiency and reliability.[30]

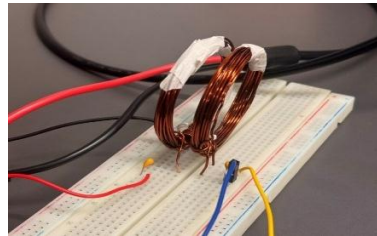Next are the breadboard connections, soldering board layout, and output waveform of the Colpitts oscillator.

Figure VI.4 Hand Coil Transformer Test

Frequency		Vrms (V)	Irms(μA)	Power(μW)	Efficiency (%) η = (Power out / Power in) +100%
10kHz	Input	0.213	2130	4536.9	0.000248
	Output	0.075	0.15	0.01125	
30kHz	Input	1.15	301	346.15	0.050845
	Output	0.8	0.22	0.176	
50kHz	Input	2.48	13.2	32.736	2.181085
	Output	3.4	0.21	0.714	
70kHz	Input	4.55	8.2	37.31	3.377111
	Output	7	0.18	1.26	
80kHz	Input	5.03	3.1	15.593	9.068172
	Output	10.1	0.14	1.414	
90kHz	Input	5.78	2.1	12.138	22.491349
	Output	13	0.21	2.73	
100kHz	Input	6.75	1.9	12.825	23.157895
	Output	13.5	0.22	2.97	
110kHz	Input	7.23	1.4	10.122	16.597510
	Output	12	0.14	1.68	
120kHz	Input	7.98	0.9	7.182	15.873016
	Output	9.5	0.12	1.14	
130kHz	Input	8.2	0.8	6.56	14.466463
	Output	7.3	0.13	0.949	
150kHz	Input	7.51	0.6	4.506	13.204616
	Output	3.5	0.17	0.595	

Table VI.1 Boost Converter Efficiency in Different Frequency
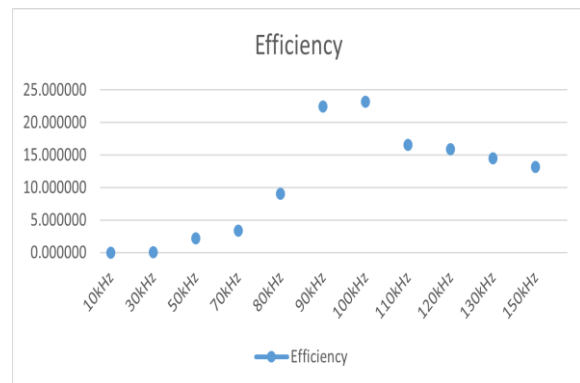

Figure VI.5 Frequency versus Power Efficiency Graph

Based on the analysis of the graphs and data, it was found that when the frequency is around 100 kHz, the Colpitts oscillator achieves a relatively high efficiency of approximately 23%. This result indicates that at this frequency, the Colpitts oscillator can minimize energy loss, but it has not yet reached the ideal energy transfer efficiency. This is partly related to the type of coil, its properties, and the winding method.[31]

In the re-work of the project, it was realized that the hand-wound coil is not efficient enough to provide substantial power for wireless power transfer. After much experimentation with different coils (varying in size and number of turns), the issue remains unresolved. This may be a key area that needs improvement in the future.

Next are the breadboard connections, soldering board layout, and output waveform of the Colpitts oscillator.
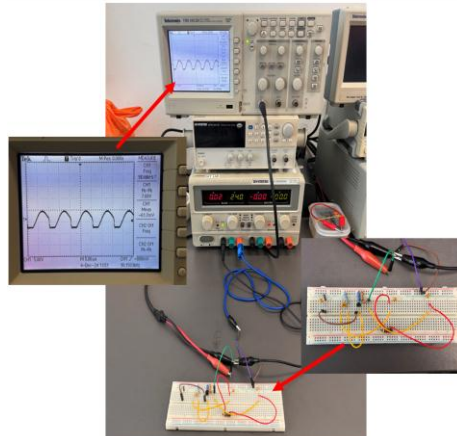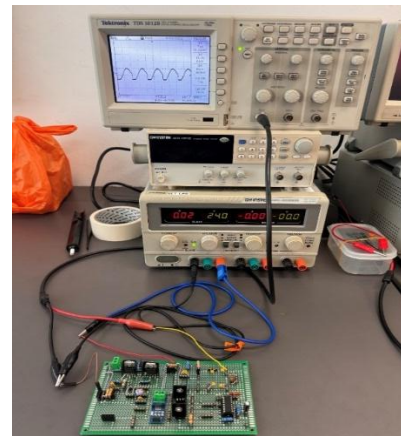

Figure VI.6 Colpitts Oscillator Bread Board Test

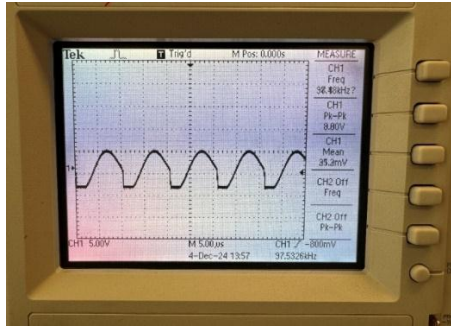Figure VI.7 Boost Converter Overall Circuit Test
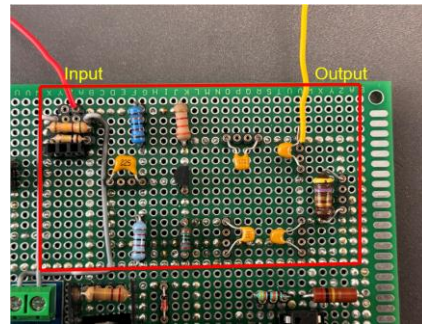
Figure VI.8 Colpitts Oscillator Output Waveform

Figure VI.9 Boost Converter Soldering Board Layout

Testing of Operational Amplifier

When connecting the oscillator to other circuits, an operational amplifier (op-amp) amplifier was installed to prevent loading effects and signal degradation.

The op-amp acted as a buffer, ensuring that the oscillator's output signal remains stable and unaffected by the impedance of the connected circuits. This prevented any unwanted attenuation or distortion of the signal, maintaining the integrity of the oscillator's performance. In this project, the output waveform from the op-amp was designed to be twice the size of the input. Therefore, the feedback resistor was chosen to be twice the value of the input resistor.
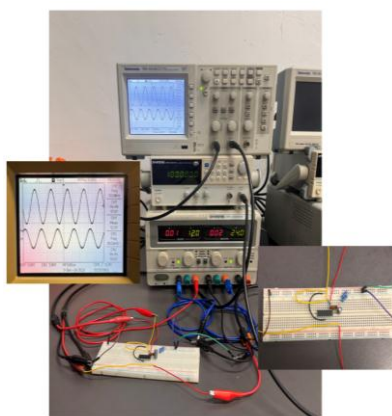

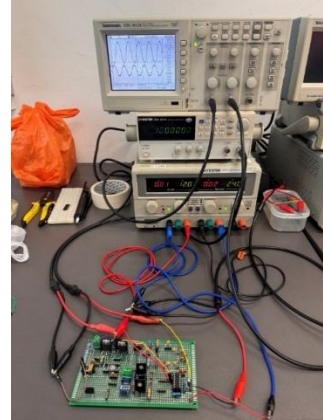Figure VI.10 Operational Amplifier Bread Board Test

Figure VI.11 Operational Amplifier Overall Circuit Test

In this design, LF347N operational amplifier was used, which has a specified operating voltage range of ±18V. However, the designed system operated with a 24V single supply, which did not fall within the required voltage range for the LF347N to function correctly. Thus, an offset circuit was implemented to adjust the input voltage levels to acceptable operating range for LF347N, set at 10Vpp with a +12V offset. This adjustment ensured that op-amp functioned correctly with the 24 single supply.
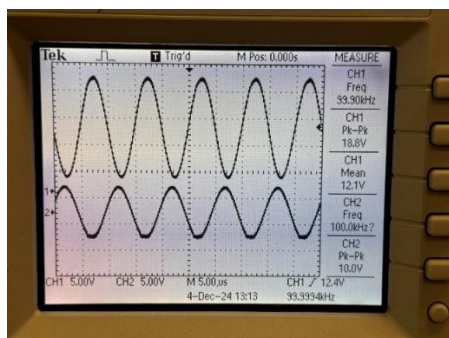

Figure VI.12 Operational Amplifier Output Waveform

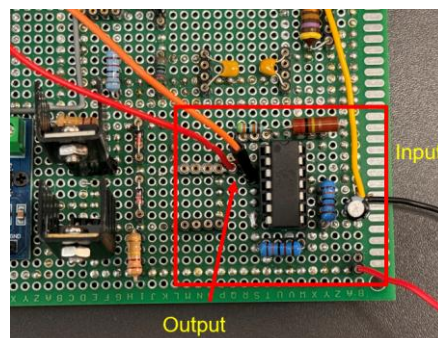Figure VI.13 Operational Amplifier Board Layout

Testing of Class AB Amplifier

The AB-class amplifier received the signal transmitted from the operational amplifier (op-amp) and amplified it to a higher current for further processing. This amplification process increased the signal's strength to meet the power requirements of the following components, ensuring the system operated successfully.
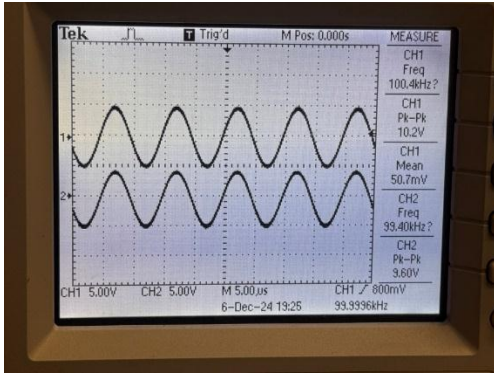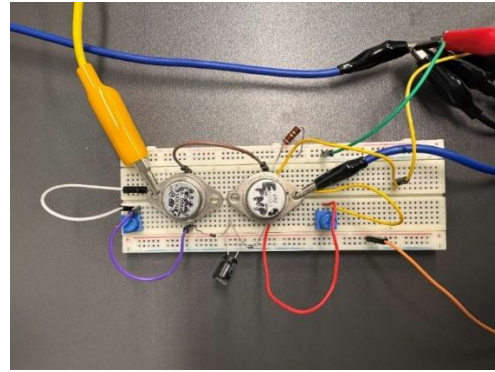
Figure VI.14 Class AB Output Waveform

Figure VI.15 Class AB Soldering Board Layout

The combination of the op-amp's signal and the AB-class amplifier's current amplification enhanced the signal. The system ensured that the transmitted signal was strong enough to effectively drive the wireless charging process, whether for charging a smartphone or powering other devices that required efficient and stable energy delivery. From Figure VI.14, the output signal of class ab amplifier is same as the input signal from op-amp.

Testing of Full Wave Rectifier
The full-wave rectifier was connected to the secondary side of the transformer, where it converted the AC voltage into a DC voltage. To evaluate the performance of the rectifier under different conditions, simulation tests were conducted with two distinct setups: one with a load capacitor and one without.

The addition of a load capacitor was expected to smooth the rectified DC output by reducing the ripple voltage, thus providing a more stable DC signal. On the other hand, the setup without a load capacitor allowed for observing the natural behavior of the rectifier without any filtering effect, which typically resulted in higher ripple and less stable DC output.

The following experimental data presents the results from both configurations, including measurements of output voltage, ripple, and other relevant parameters.
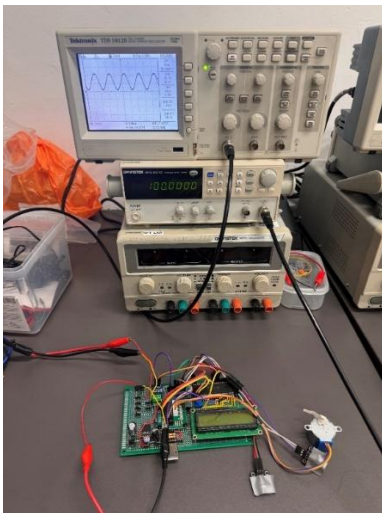

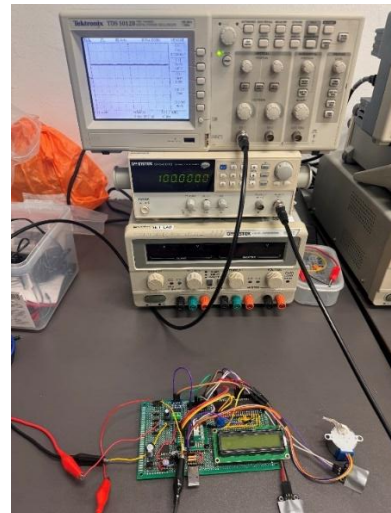Figure VI.16 Full Wave Rectifier without Load Capacitor Test

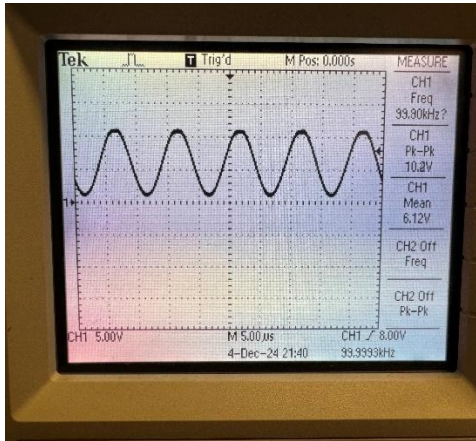Figure VI.17 Full Wave Rectifier with Load Capacitor Overall Circuit Test

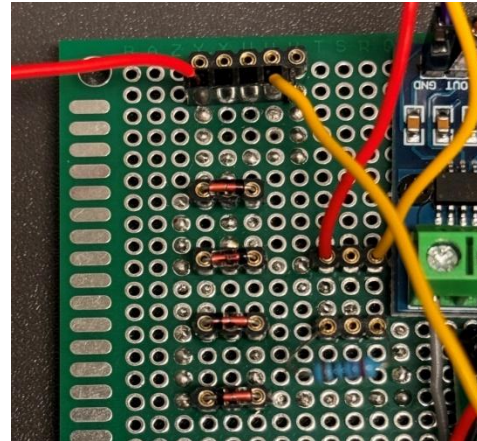Figure VI.18 Full Wave Rectifier without Load Capacitor

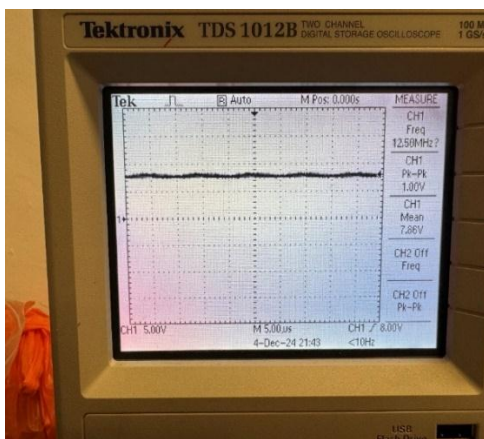Figure VI.19 Full Wave Rectifier without Load Capacitor Board Layout

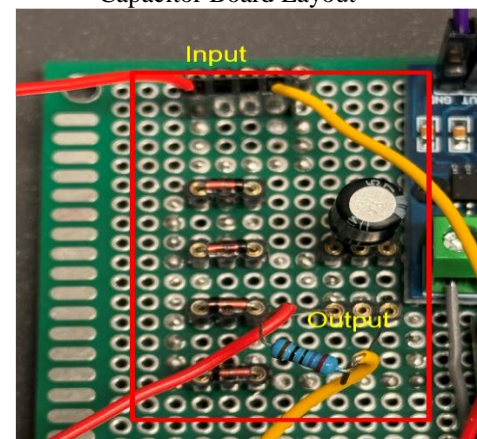Figure VI.20 Full Wave Rectifier with Load Capacitor

Figure VI.21 Full Wave Rectifier with Load Capacitor Soldering Board Layout

Through the comparison of both configurations, adding a load capacitor resulted in a much smoother output. The load capacitor successfully converted the AC input into a stable DC output. Therefore, adding the load capacitor was the better choice for achieving a more reliable and efficient DC power supply.

Testing of Buck Converter
In the previous design of the buck converter, efficiency obtained was only around 70%. The low efficiency was attributed to the significant power losses in the discrete components used in the circuit, including the MOSFETs, inductors, and capacitors. These losses were mainly due to factors like switching losses, conduction losses, and imperfect component characteristics. As a result, the converter was not performing optimally due to undesired output voltage and current without sufficient efficiency.

Therefore, a buck converter IC (LM2596) was applied to replace the discrete components. This was because the specialized IC was designed for high efficiency with optimized internal circuitry that reduced power losses. This solution not only improved the efficiency closer to 90%, but it also reduced the complexity of the circuit, and the number of external components required.

With the new buck converter IC (LM2596), expected output of 5V and 1A were achieved. The integrated design of the IC also ensured better thermal management and more stable performance, resulting in an efficient power supply. In addition, it also ensured a better performance of the entire system and easier implementation in the application.
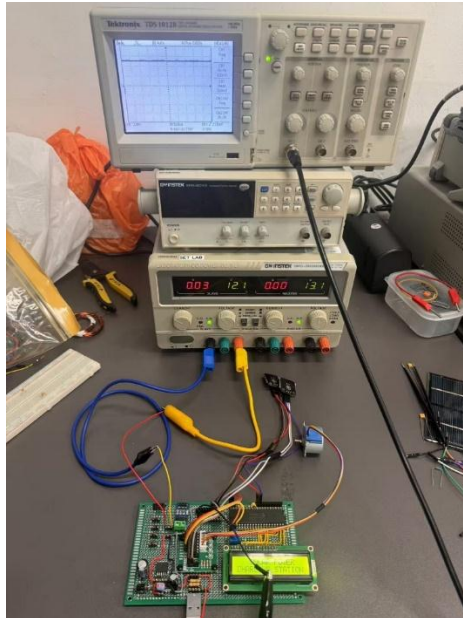
Figure VI.22 Buck Converter Overall Circuit Test
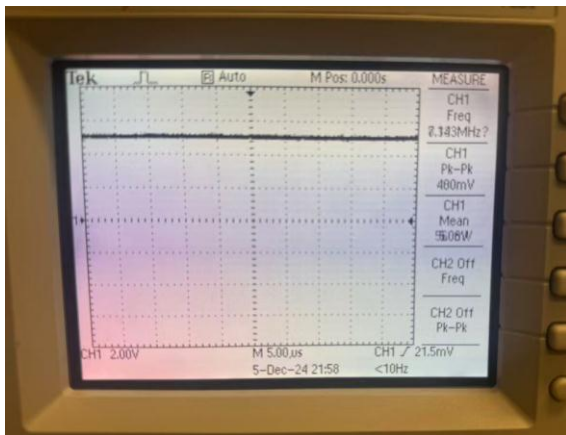
Figure VI.23 Buck Converter Output Waveform
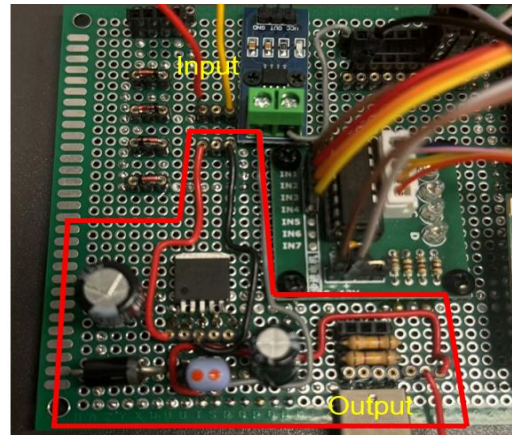
Figure VI.24 Buck Converter Soldering Board Layout

Solar Panel Testing[32]

The efficiency of the solar panel is an important part of this project. The testing was conducted in a dark environment with only one light source. The selected solar panel has an output voltage of 12V. During the test, the solar panel was placed 20 cm away from the light source to begin with. It was observed that the closer the solar panel was to the light source, the stronger the output current. Below are the output voltage and current data obtained by moving the solar panel to different positions:

Figure VI.25 Solar Panel Test with Moving from 20cm Hight

Distance from light (cm)	V_{out} (V)	I_{out} (mA)
20	12.25	0.012
15	12.33	0.053
10	12.28	0.097
5	12.17	0.167
3	12.34	0.189

Table VI.2 Output Voltage and Current of Different Placing of Solar Panel

Based on the test data, it can be observed that the closer the solar panel is to the light source, the lighter it absorbs, leading to higher photoelectric conversion efficiency. This is because a greater amount of light reaches the surface of the solar panel when the distance between the panel and the light source is smaller. Consequently, more energy is converted into electrical energy, improving the overall efficiency of the solar panel.

Figure VI.26 Testing of Solar Panel with Different Angles

Similarly, when the solar panel and the light source are positioned at an angle to each other, there is a noticeable loss in photoelectric conversion efficiency. This occurs because the light does not hit the surface of the solar panel perpendicularly, causing less light to be absorbed. As a result, the amount of energy converted into electricity decreases, which leads to a reduction in the solar panel's efficiency. This highlights the importance of optimizing the alignment of the solar panel with respect to the light source to maximize its performance.[34]

In the subsequent MCU design, a motor and a light sensor will be integrated to enable dynamic adjustment of the solar panel's angle. The motor will control the rotation of the panel, while the light sensor will monitor the light intensity and direction, adjusting the angle in real time to ensure the panel receives maximum light. By rotating the panel to ensure perpendicular light exposure, the system will optimize photoelectric conversion efficiency, reduce energy loss due to misalignment, and improve the overall performance of the solar power system.

It is possible to increase the output current and power by connecting solar panels in parallel while keeping the output voltage constant. In practical testing, due to the limitations of the laboratory, only one solar panel was used for testing. However, by connecting multiple solar panels in parallel, it is possible to provide power to the circuit and ensure that all components operate properly.

Overall Circuit Testing
After connecting all the components and performing thorough debugging, the final charging circuit was successfully set up as follows:
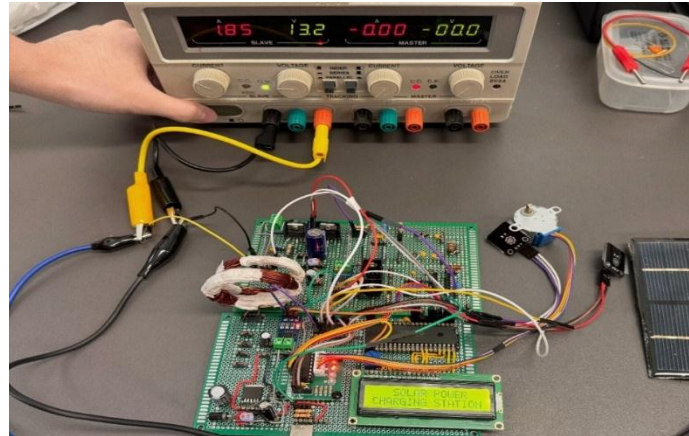
Figure VI.27 Overall Charging Circuit Test
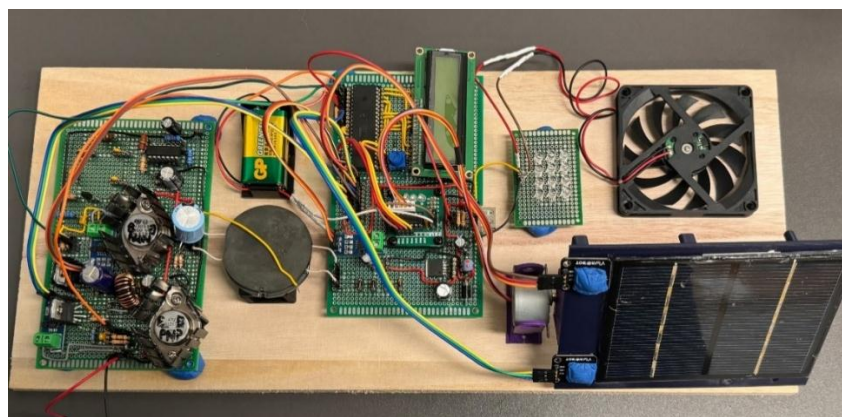
Figure VI.28 Final Output Group of LEDs and Fan

A 12V DC input was provided. The circuit regulated and converted the input voltage to output of 4.43V, which was an acceptable output. And output current detected was 0.27A. This output was suitable for supplying all the LEDs and able to power the fan.

In addition, the circuit was versatile enough to power small electronic devices like low-power equipment. The design successfully integrated the solar energy input with the battery backup, making it a reliable solution for portable and wireless power applications.

VII.   MCU Testing

Light Sensor, Motor [19] and Current Sensor
Two light sensors were positioned on opposite sides of the solar panel to continuously monitor the light intensity on each side. These sensors can detect the variations in sunlight and provide real-time feedback on which side of the solar panel was receiving more light. By comparing the light intensity data from both sensors, the system can control which direction the solar panel should face to optimize sunlight exposure.

Figure VII.1 Light Sensors Connection

Figure VII.2 Stepper Motor Connection

A stepper motor was mounted on one side of the solar panel, and it was responsible for adjusting the panel's angle. The motor was control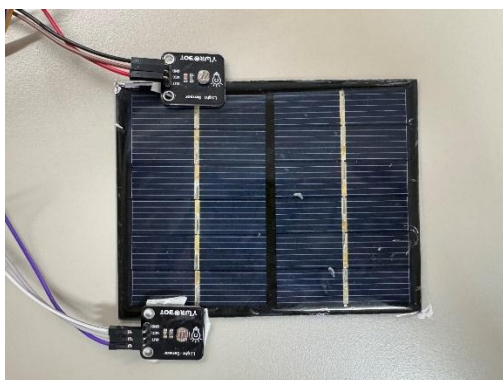led by the light sensors, rotating the panel to the optimal position based on which side was receiving more sunlight. This automatic adjustment ensured that the solar panel always maintained the best angle for capturing the maximum amount of solar energy.[39]

The aim of this design was to maximize the solar panel's exposure to sunlight, which resulted in increasing the effective surface area exposed to light and improved the overall energy conversion efficiency. By constantly adjusting the angle of the panel, the system optimized the solar panel's performance, ensuring that it can generate the maximum power output throughout the day.

The 19CXYH8K stepper motor driver IC was used to control and drive the stepper motor. Under normal operating conditions, the driver IC operates at a supply voltage of 5V with a current consumption of 0.32A. This allowed the stepper motor to rotate smoothly and accurately based on input signals from the MCU.

Despite the addition of the stepper motor and the driver IC to the circuit, the overall system continued to meet its current supply requirements. The power supply can deliver enough current to support the entire system, including the MCU, sensors, LCD display, and the stepper motor driver.
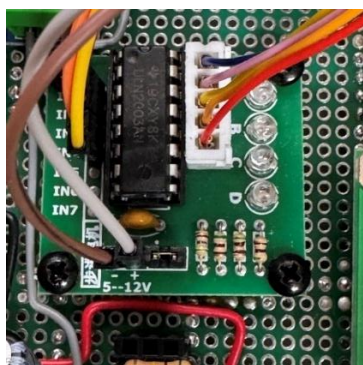

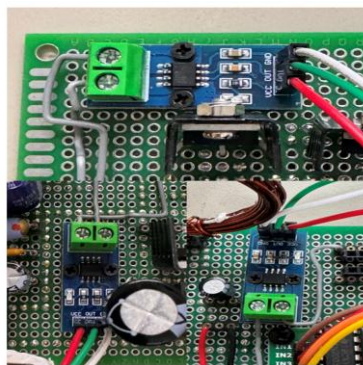Figure VII.3 Stepper Motor Driver 19CXYH8K

Figure VII.4 Current Sensors Connection

Three current sensors were installed at the power input of the charging device, the output of the boost converter, and the final output of the charging device. These sensors continuously monitor the current in each section and transmit the data to the MCU. The real-time current readings are displayed on the LCD, allowing users to easily monitor the status of each part of the system. If any abnormalities are detected, timely adjustments can be made to ensure optimal performance and prevent potential issues.

MCU[25]

The MCU (PIC18F4550) is responsible for receiving, processing, and outputting information within the system. It plays a crucial role in monitoring various parameters, including voltage levels from different parts of the circuit, and displaying real-time data on the LCD. However, the input voltage to the MCU must remain within its rated input range of 3.3V to 5V to ensure proper operation and prevent potential damage to the microcontroller.

To maintain accurate and reliable voltage readings, voltage divider circuits are implemented at each voltage measurement point throughout the system. These voltage divider circuits ensure that the voltages into the MCU are consistently within the range. By adjusting and regulating the input voltages, the voltage divider circuits effectively protect the MCU from any voltage spikes or fluctuations that could fall outside its input range.

In this setup, the MCU can process the received data, making precise decisions based on the monitored voltages, such as adjusting the charging process, controlling the stepper motor for solar panel position. This ensures the system operates efficiently and safely while allowing the MCU to output information to the LCD, providing real-time feedback on the performance of the system.[40]

Then clear the display on the LCD, then display the 'MOTOR RUNNING' signal. After that, read the data from AN6 and AN7 (Light Sensor 1 and Light Sensor 2) for subsequent processing.

Figure VII.5 LCD Display 'SOLAR POWER CHARGING STATION'

Figure VII.6 LCD Display 'MOTOR RUNNING'

Clear the display on the LCD, then display the 'MOTOR RUNNING' signal. After that, read the data from AN6 and AN7 (Light Sensor 1 and Light Sensor 2) for subsequent processing.

Next determines the rotation of the stepper motor by comparing the data from two light sensors. When the light intensity of Light Sensor 1 is greater than that of Light Sensor 2, the motor will rotate clockwise. Conversely, if the light intensity of Light Sensor 2 is greater, the motor will rotate counterclockwise.

| Figure VII.7 Stepper Motor Initial Direction | Figure VII.8 Stepper Motor Turns Clockwise (AN6<AN7) | Figure VII.9 Stepper Motor Turns Anticlockwise (AN6>AN7) |

Clear the LCD Display and initialize SPV (Solar Panel Voltage) and start reading the Input voltage (AN0). The range of ADC reading is 0 – 1023. With the reference voltage set to 5V. The voltage for each step size is calculated. By using the formula and the ratio of voltage divider circuit, SPV can be calculated, and it displayed on the LCD. Then clear the LCD Display and initialize SPC (Solar Panel Current) and start reading the Input voltage (AN1). The current sensor measures current when it reached 2.5V, each 0.18V above the threshold corresponds to 1A.SPC can be calculated, and it displayed on the LCD. Readings below 2.5V will not be considered, and the display will show 0A

| Figure VII.10 LCD Display the Voltage of Solar Panel | Figure VII.11 LCD Display the Current of Solar Panel |

After the LCD displays the current from the buck converter, MCU returns to reading and comparing the values of AN0 and AN1 and keeps looping. However, when the values from AN0 and AN1 are equal, the LCD does not display the 'MOTOR RUNNING' message. Instead, it will directly continue displaying the voltage and current values of the various test points. This behavior is achieved by using an 'if' condition and a 'while' loop.

Reference

[1]. J. Khan, M.H. Arsalan / Renewable and Sustainable Energy Reviews 55 (2016) 414–425
[2]. G. Boyle. *Renewable Energy: Power for a Sustainable Future*, 2nd ed. Oxford, UK: Oxford University Press, 2004.
[3]. Green, M. A., Dunlop, E. D., Yoshita, M., Kopidakis, N., Bothe, K., Siefer, G., & Hao, X. (2023). Solar cell efficiency tables (version 62). *Progress in Photovoltaics: Research and Applications*. Doi:10.1002/pip.3726
[4]. Hasaneen, B. M., & Elbaset Mohammed, A. A. (2008, March 1). *Design and simulation of DC/DC boost converter*. IEEE Xplore. https://doi.org/10.1109/MEPCON.2008.4562340
[5]. Spohr, S. (n.d.). *Understanding Power Inductor Parameters*. Retrieved August 1, 2024.
[6]. Aldair, A. A., Obed, A. A., & Halihal, A. F. (2018). Design and implementation of ANFIS-reference model controller based MPPT using FPGA for photovoltaic system. *Renewable and Sustainable Energy Reviews*, *82*, 2202–2217.
[7]. Kazimierczuk, M., & Murthy-Bellur, D. (2010). Loop Gain of the Common-Drain Colpitts Oscillator. *International Journal of Electronics and Telecommunications*, *56*(4), 423–426.
[8]. *Design and simulation of DC/DC boost converter*. (2008, March 1). IEEE Conference Publication | IEEE Xplore.
[9]. Maggio, G.M., O. De Feo and Kennedy, M.P. (1999). Nonlinear analysis of the Colpitts oscillator and applications to design. *IEEE transactions on circuits and systems*, 46(9), pp.1118–1130
[10]. Pillay, S. and Srivastava, V.M. (2020). Realization with Fabrication of Double-Gate MOSFET Based Class-AB Amplifier. *International Journal of Electrical and Electronic Engineering & Telecommunications*, pp.399–408.

[11]. Ejury, J. (2013). *Buck Converter Design*. [online] Available at: https://cdn.badcaps-static.com/pdfs/2a997c023d0eda74b0a3c42d4b38ca9c.pdf.

[12]. Zhang, Z., Pang, H., Georgiadis, A. and Cecati, C. (2019). Wireless Power Transfer—An Overview. *IEEE Transactions on Industrial Electronics*, [online] 66(2), pp.1044–1058.

[13]. Al-Ezzi, A.S.; Ansari, M.N.M. Photovoltaic Solar Cells: A Review. Appl. Syst. Innov. 2022, 5, 67. https://doi.org/10.3390/asi5040067

[14]. Askari Mohammad Bagher, Mirzaei Mahmoud Abadi Vahid, Mirhabibi Mohsen. Types of Solar Cells and Application. American Journal of Optics and Photonics. Vol. 3, No. 5, 2015, pp. 94-113. doi: 10.11648/j.ajop.20150305.17

[15]. Kok, C.L.; Tang, H.; Teo, T.H.; Koh, Y.Y. A DC-DC Converter with Switched-Capacitor Delay Deadtime Controller and Enhanced Unbalanced-Input Pair Zero-Current Detector to Boost Power Efficiency. Electronics 2024, 13, 1237. doi: 10.3390/electronics13071237

[16]. Woywode, O.; Güldner, H. "Application of Statistical Analysis to DC-DC Converter" International Power Electronics Conference, IPEC 2000, Tokyo, Japan 2000.

[17]. Toumazou, C., Lidgey F. J. and Chattong S., High frequency current conveyor precision full-wave rectifier, Electronics Letters, vol. 30, No.10, pp. 745– 746, 1994.

[18]. Ramakant A.Gayakwad, "Op-Amps and linear integrated Circuits"

[19]. Kok, C.L.; Dai, Y.; Lee, T.K.; Koh, Y.Y.; Teo, T.H.; Chai, J.P. A Novel Low-Cost Capacitance Sensor Solution for Real-Time Bubble Monitoring in Medical Infusion Devices. Electronics 2024, 13, 1111. doi: 10.3390/electronics13061111

[20]. AN166 - Basic Feedback Theory, Philips Semiconductors Application Note, Dec 1988 Opamps For Everyone - by Ron Mancini, Editor in Chief, Texas Instruments, Sep 2001

[21]. Maggio, G.M., De Feo, O., Kennedy, M.P., 1999. Nonlinear analysis of the Colpitts oscillator and applications to design, IEEE Transactions on Circuits and Systems I: Fundamental Theory and Applications, 46 (9), pp.1118-1130, Sep 1999.

[22]. Imani A, Hashemi H. Frequency and power scaling in mm-wave Colpitts oscillators. IEEE J Solid State Circuits. 2018; 53(5): 1338-1347.

[23]. G. Giustolisi, G. Palumbo, and S. Pennisi, "Class-AB CMOS output stages suitable for low-voltage amplifiers in nanometer technologies," Microelectronics Journal, vol. 92, pp. 1-7, Oct. 2019.

[24]. B. Cordell, Designing Audio Power Amplifiers, 1st Ed., McGraw Hill, 2010.

[25]. Kok, C.L.; Ho, C.K.; Lee, T.K.; Loo, Z.Y.; Koh, Y.Y.; Chai, J.P. A Novel and Low-Cost Cloud-Enabled IoT Integration for Sustainable Remote Intravenous Therapy Management. Electronics 2024, 13, 1801. doi: 10.3390/electronics13101801

[26]. C.-Y. Lin, C.-H. Tsai, H.-T. Lin, L.-C. Chang, Y.-H. Yeh, Z. Pei, et al., "High-frequency polymer diode rectifiers for flexible wireless power-transmission sheets", *Org. Electron.*, vol. 12, no. 11, pp. 1777-1782, Nov. 2011.

[27]. Wikipedia, the Free Encyclopedia, DzBuck Converter (online), Available from http://en.wikipedia.org/wiki/Buck converterdz

[28]. Robert W. Erickson and Dragon Maksimoni, DzFundamentals of Power Electronicsdz. SECOND EDITION, Springer International Edition.

[29]. Detka, K.; Górecki, K.; Ptak, P. Model of an Air Transformer for Analyses of Wireless Power Transfer Systems. Energies 2023, 16, 1391. https://doi.org/10.3390/en16031391

[30]. Okoyeigbo, O.; Olajube, A.; Shobayo, O.; Aligbe, A.; Ibhaze, A. Wireless power transfer: A review. IOP Conf. Ser. Earth Environ. Sci. 2021, 655, 012032. [CrossRef]

[31]. Rim, C.T.; Mi, C. Wireless Power Transfer for Electric Vehicles and Mobile Devices; John Wiley and Sons: West Sussex, UK, 2017

[32]. Ahiska, R., Nykyruy, L., Omer, G., and Mateik, G. (2016). The Thermoelectric Solar Panels. jpnu 3 (1), 9–14. doi:10.15330/jpnu.3.1.9-14

[33]. J. Kong, L. Siek and C. L. Kok, "A 9-bit body-biased vernier ring time-to-digital converter in 65 nm CMOS technology," 2015 IEEE International Symposium on Circuits and Systems (ISCAS), Lisbon, Portugal, 2015, pp. 1650-1653, doi: 10.1109/ISCAS.2015.7168967.

[34]. Al-Waeli, A. H., Sopian, K., Kazem, H. A., and Chaichan, M. T. (2016). Photovoltaic Solar Thermal (PV/T) Collectors Past, Present and Future: A Review. Int. J. Appl. Eng. Res. 11 (22), 10757–10765.

[35]. A. Kurs, A. Karalis, R. Moffatt, J. D. Joannopoulos, P. Fisher, and M. Soljacˇ c, "Wireless power transfer via strongly coupled magnetic reso- ´ nances," Science, vol. 317, no. 5834, pp. 84–86, 2007

[36]. Liu S, Dougal RA. Dynamic multiphysics model for solar array. IEEE Trans Energy Convers 2002;17(2):285–94.

[37]. Bryan F. Simulation of grid-tied building integrated photovoltaic systems. MS thesis, Solar Energy Laboratory, University of Wisconsin, Madison, 1999.

[38]. Electronicwings Interfacing LCD 16x2 in 4-bit mode with PIC18F4550 https://www.electronicwings.com/pic/interfacing-lcd-16x2-in-4-bit-mode-with-pic18f4550-

[39]. F. A. Kazan, A. C. AÄŸaçayak, C. Arslan and M. Selek, MikroC jle PIC18F4550 Uygulamalari, Konya:Mesleki Akademi, 2014.

[40]. M. T. Inc, "PICDEM™ PIC18 Explorer Demonstration Board User's Guide", 2008.

[41]. C. Ma, Q. Li, Z. Liu and Y. Jin, "Low cost AVR microcontroller development kit for undergraduate laboratory and take-home pedagogies", *Education Technology and Computer (ICETC) 2010 2nd International Conference on*, pp. Vl-35-Vl-38, 2010.